

Crystal contacts engineering of aspartyl-tRNA synthetase from *Thermus thermophilus*: effects on crystallizability

Christophe Charron, Daniel Kern and Richard Giegé

Département 'Mécanismes et Macromolécules de la Synthèse Protéique et Cristallogénèse', UPR 9002 'Structure des Macromolécules Biologiques et Mécanismes de Reconnaissance', Institut de Biologie Moléculaire et Cellulaire du CNRS, 15 rue René Descartes, 67084 Strasbourg Cedex, France. E-mail: R.Giege@ibmc.u-strasbg.fr

To understand how surface residues in a protein structure influence crystal growth, packing arrangement and crystal quality, crystal surfaces were modified and crystallizability of seven different mutants investigated. The model was aspartyl-tRNA synthetase-1 from *Thermus thermophilus*, a homodimer (M_r 122,000) with a subunit of 580 amino acids. Engineering concerned modification of amino acids involved in packing contacts in the orthorhombic lattice ($P2_12_12_1$) of the synthetase. Comparison of the crystallization behaviour of the mutants indicates a correlation between disruption/addition of packing interactions and crystallizability of the mutants: disruption or modification of lattice contacts prevents crystallization or leads to crystals of poor quality. In contrast, addition of potential contacts leads to well-shaped crystals of same space group and cell parameters than wild-type crystals.

Keywords: aspartyl-tRNA synthetase, crystal engineering, crystal packing

1. Introduction

Proteins and other biomacromolecules have the natural potential to interact via hydrogen bonds, ionic and Van der Waals contacts. Such contacts are precisely those occurring in intermolecular packing within macromolecular crystals. Even if protein crystallization seems to depend predominantly on random protein-protein interactions, which have little in common with physiological protein-protein recognition processes (Carugo & Argos, 1997; Janin, 1997), such contacts may have biological relevance, especially in macromolecular self-assembly processes. Here, the aim is to understand how surface residues in an aminoacyl-tRNA synthetase structure influence crystal growth, packing arrangement and crystal quality, and to investigate how engineering crystal surfaces modifies crystal properties.

There are a few examples of crystal contact engineering in the literature. One commonly quoted example is that of human H-chain ferritin (Lawson *et al.*, 1991). While the related rat and horse L-chain ferritins give good crystals, the human protein gives poor crystals under the same crystallization conditions. Examination of the crystal contact regions of these ferritins, crystallized in the presence of Cd^{2+} ions, readily indicated why human H-chain ferritin failed to crystallize. Indeed, the horse and rat ferritin molecules are linked together by double Cd^{2+} bridges in the crystalline lattice. Introducing the K86Q mutation at the surface of the human protein

enabled this metal bridge to form in the crystals that now diffracted to 1.9 Å resolution and allowed determination of the three-dimensional structure of the human protein. Likewise, crystal engineering of canavalin showed that a mutant (R301E) designed to disrupt an intermolecular salt-bridge interaction with D107 produces crystals of higher overall quality (Green *et al.*, 2001) due to the formation of an intermolecular metal bridge involving E301 and D107. Another example of crystal contact engineering is T4 lysozyme where the introduction of a disulfide bridge between two molecules hastens nucleation, promotes crystal growth and reduces threefold the crystallization time (Heinz & Matthews, 1994). On the other hand, a variant of the enzyme glutathione reductase was designed in order to form two additional hydrogen bonds in crystal contacts (Mittl *et al.*, 1994). Although the double mutation had no direct effect on molecular packing and resolution limit of the X-ray diffraction, it facilitated crystal nucleation dramatically and shortened the crystallization time by a factor of forty. The intrinsic solvation properties of human thymidylate synthase were altered with the aim to improve crystallizability (McElroy *et al.*, 1992). Mutations were such to change the charge or polarity of surface amino acids. As a result, some mutants showed enhanced crystallizability, others gave crystals under novel conditions or of different space groups than the wild-type crystals. From another perspective, human insulin crystal were engineered for being used as more efficient pharmaceutical preparations (Berchtold & Hilgenfeld, 1999). Many proteins, mainly of eukaryotic origin and of multidomain architecture, cannot be crystallized because of structural flexibility. The better crystallization of proteolytic fragments or engineered protein cores compared with the whole molecules from which they derive shows that extra domains can hinder crystallization (e.g. Waller *et al.*, 1971; Bergfors *et al.*, 1989; Bourguet *et al.*, 1995). Related to this work, we mention the case of yeast aspartyl-tRNA synthetase that initially yielded poor and anisotropic diffracting crystals. Crystal quality could be improved by removing the 70 amino acid long N-terminal extension of the protein (Sauter *et al.*, 2000). Examination of the crystal lattice indicated an intermolecular contact that is perturbed in the protein with the floppy appendix, explaining thereby the poor quality of the wild-type crystals (Sauter *et al.*, 2001).

In this paper, the model protein is aspartyl-tRNA synthetase (AspRS-1) from *Thermus thermophilus* whose structure is known in an orthorhombic (Delarue *et al.*, 1994; Ng *et al.*, 2002) and a monoclinic (Charron *et al.*, 2001) space group. Based on an analysis of the orthorhombic crystals (Charron *et al.*, 2001), seven variant proteins were produced with mutations at contact positions in the orthorhombic lattice. They present modified charge distribution at their surface, modified local surface hydrophobicity or perturbed H-bonding patterns involved in crystal contacts. The comparison of the crystallization of these mutants highlights a correlation between disruption/addition of intermolecular interactions in crystal packing and crystallizability.

2. Experimental procedures

2.1. Mutagenesis, expression and purification

All mutants were constructed in the wild-type AspRS-1 gene (Becker *et al.*, 2000) by using site-directed mutagenesis (Kunkel, 1985) on single-stranded M13mp18 recombined with the 4.5 kbp *Bam*HI fragment. The R28E, A53I, R160E, E161R, E355R, S360A and F366A mutants were produced using the mutagenic oligonucleotides 5'GGGTCAACCGCGAGCGCGACCTCCGCCGC GCGACCTCGGCGGC3', 5'GGCCACCCCAATTAGCCCCGCC3', 5'GGGACTTCTGGACGAGGAGGGCTTCG3', 5'GGGACTTC

CTGGACCGGGCGGGGCTTCGTCAA3', 5'TGGGCCCGGGTGCG GGAGGAGGGGGGTT3', 5'GAGGGGGGGTTCGCGGGGGTG TGGCC3', and 5'CGGGGGTGTGGCCAAGGCTTTAGAACCCGT G3', respectively. The mutation sites (in italics) were controlled by sequencing. The *EcoRI-HindIII* fragments were excized from recombinated M13mp18, cloned in pKK223 expression vectors and the resulting vectors were used for transformation of *E. coli* strain JM103. The mutants were overexpressed and purified like native protein (Becker *et al.*, 2000) and analyzed by SDS-PAGE.

2.2. Crystallization

Mutants were crystallized using conditions close to those described for the wild-type enzyme (Delarue *et al.*, 1994; Ng *et al.*, 2002) using the hanging drop method. For each mutant, the optimal crystallization condition established for the wild-type enzyme (sodium formate 3.55 M at pH 6.9) was tested, plus a set of 12 other conditions (2.3, 2.5, 2.7, 2.9, 3.1, 3.3, 3.5, 3.7, 3.9, 4.1, 4.3, and 4.5 M sodium formate at pH 6.9). Reservoir solution (4 μ l) was mixed with 4 μ l protein solution (10 mg/ml) in 20 mM Tris-HCl buffer, 0.5 mM EDTA and 5 mM β -mercaptoethanol at pH 7.5. Crystallization experiments were performed at 293 K.

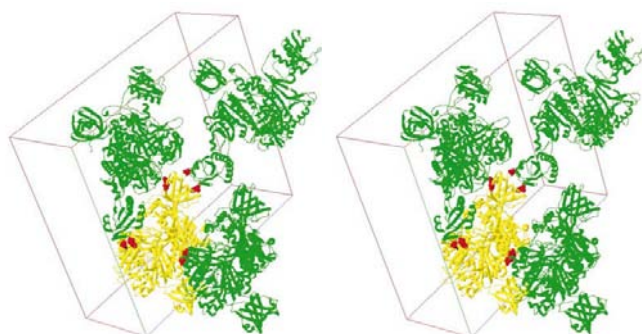


Figure 1

Mutated residues (spheres) involved in packing contacts in orthorhombic crystals of aspartyl-tRNA synthetase from *T. thermophilus*.

2.3. X-ray diffraction analysis

Prior to data collection, crystals were soaked for about 20 s in a cryoprotectant composed of reservoir solution of crystallization mixed with 20% (v/v) glycerol. Crystals were then mounted in a nylon loop and flash-cooled in liquid ethane at 120 K. X-ray data were collected at 100 K on a DIP2000 Enraf-Nonius area detector using a rotating-anode generator (wavelength 1.542 Å, crystal-to-detector distance 160 mm). X-ray patterns were indexed and cell parameters were defined using *DENZO* (Otwinowski & Minor, 1996).

2.4. Design of mutants

In the orthorhombic crystals of AspRS-1 from *T. thermophilus*, 14.4% (7040 Å²) of the total accessible surface of the protein is involved in crystal contacts (Charron *et al.*, 2001) and three types of contacts occurring twice are found with buried surfaces of 1770 Å², 1020 Å² and 730 Å², respectively. Mutation sites at the protein surface were chosen in order to modify different kinds of intermolecular interactions (Table 1).

Mutants R160E, R28E, E161R and E355R were designed to analyze the effect of ionic interactions on crystallizability. The influence of hydrophobic contacts in crystallizability was analyzed with A53I and F366A mutants, while mutant S360A was aimed to see the consequences on crystallization of the disruption of a hydrogen bond.

Figure 1 shows the localization of the seven mutations at packing contacts in the orthorhombic crystal lattice of dimeric AspRS-1. These mutations are distributed in the three different types of contact surfaces occurring in the orthorhombic crystals. Three of them (R28E, E355R and S360A) are in the largest buried surface, two others (R160E and E161R) are located in the smallest buried surface and the two last ones (A53I and F366A) are found in the third type of contact region. Residues R28, E355 and S360 of one AspRS-1 dimer are involved in intermolecular interactions with another dimer in the crystal, both dimers being directly related by a crystallographic 2₁ screw axis parallel to the *b* axis. Otherwise, residues R160 and R161 are involved in interactions between dimers only related by translation along the *a* axis. The third type of contact involving residues A53 and F366 corresponds to interactions between AspRS-1 dimers related by a combination of crystallographic 2₁ screw axis parallel to the *c* axis and translation along the *a* axis.

Table 1

Effect of seven different mutations on crystallization of AspRS-1 from *T. thermophilus*.

Contacts between dimers	Buried surface	Residue mutation	Contact modification	Effect on crystallization, space group ^a
$x, y, z \leftrightarrow -x, -1/2+y, 1/2-z$	2x1770 Å ²	R28E	creates ionic interaction	no crystal
$-x, 1/2+y, 1/2-z \leftrightarrow x, y, z$		E355R	disrupts ionic interaction	no crystal
		S360A	disrupts hydrogen bond	no crystal
$x, y, z \leftrightarrow -1/2-x, 1-y, z+1/2 \leftrightarrow x, y, z$	2x1020 Å ²	A53I hydrophobic contact	increases	single crystals, $P2_12_12_1^b$
$-1/2-x, 1-y, z+1/2 \leftrightarrow x, y, z$		F366A	decreases hydrophobic contact	twinned crystals, space group ND ^c
$x, y, z \leftrightarrow x-1, y, z$	2x730 Å ²	R160E	creates ionic interaction	single crystals, $P2_12_12_1^b$
$x+1, y, z \leftrightarrow x, y, z$		E161R	disrupts ionic interaction	cluster of rods, $P2_12_12_1^b$

^a Space group of wild-type AspRS-1 is $P2_12_12_1$ with parameters a=62; b=156; c=178Å.

^b Cell parameters as for wild-type.

^c ND: not determined.

3. Results and discussion

3.1. General features of wild-type and mutant crystallization

Figure 2a shows a typical crystal of wild-type AspRS-1 which grew from a precipitate. All mutants showed a similar behavior leading to protein precipitation after two hours equilibration. Four out of seven mutants form crystals (Fig. 2c,d,e,f) which all grew by

an Ostwald type ripening process as found for the wild-type protein (Ng *et al.*, 1996).

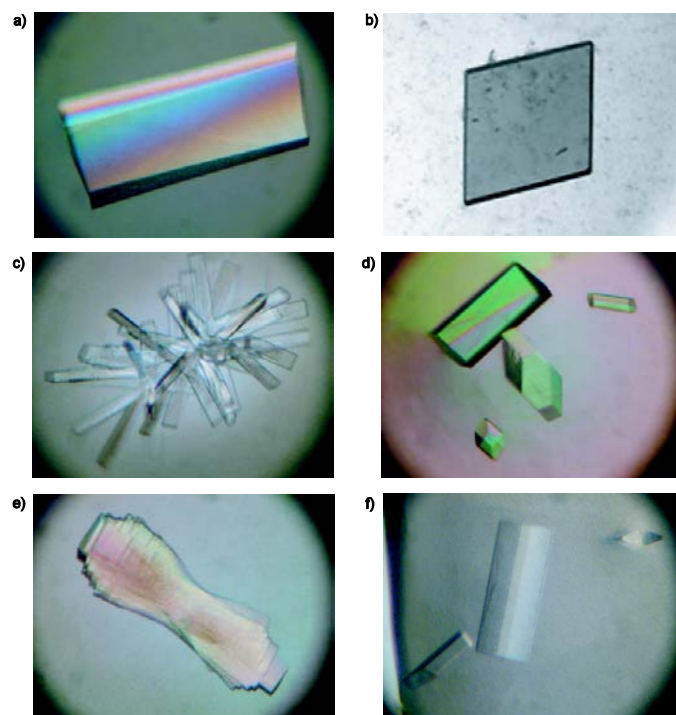


Figure 2

Crystals of wild-type AspRS-1 in (a) orthorhombic and (b) monoclinic lattices and crystals of (c) E161R, (d) R160E, (e) F366A, and (f) A531 mutants obtained using conditions close to those used for orthorhombic crystals of the wild-type enzyme.

3.2. Modification of ionic packing contacts

Crystallization of mutant E161R, where the mutation of the glutamate into an arginine residue does not allow formation of an intermolecular ionic interaction, gave clusters of rod-like crystals (Fig. 2c). Thus, the salt-bridge formed between E161 of one native AspRS-1 dimer and R579 of the other dimer seems to be important for crystallization. This salt-bridge, which is formed between dimers related only by a crystallographic translation along the *a* axis, appears to be important during the nucleation step.

Disruption of another ionic packing interaction in E355R mutant has a more drastic effect since the variant protein does not crystallize in the presence of sodium formate. In native crystals, E355 forms a double salt-bridge with R331 and R353 of a neighboring AspRS-1 dimer (Fig. 3), both dimers being directly related by the crystallographic 2_1 screw axis parallel to the *b* axis.

The R160E mutation affects one of the smaller crystal contacts. Figure 4 shows the region of the wild-type enzyme around residue R160 which is close to R571 from another AspRS-1 dimer. By introducing the mutation R160E, an unfavorable electrostatic interaction should be changed to a favorable salt-bridge. It was hoped that this additional contact would solidify the three-dimensional lattice, thereby improving the crystal order. Initial crystallization attempts with this mutant gave crystals of good optical quality in the same habit as wild-type (Fig. 2d). Crystals of the R160E grow in the orthorhombic $P2_12_12_1$ space group as wild-

type AspRS-1, with identical lattice parameters ($a = 62 \text{ \AA}$, $b = 156 \text{ \AA}$ and $c = 178 \text{ \AA}$).

Another mutant (R28E), which was engineered to add one ionic interaction in crystal contacts, does not crystallize at all. This could be explained by the formation of an intramolecular interaction between the side-chains of E28 and R64 from the same dimer rather than by the expected intermolecular ionic interaction with R64 from a neighboring dimer.

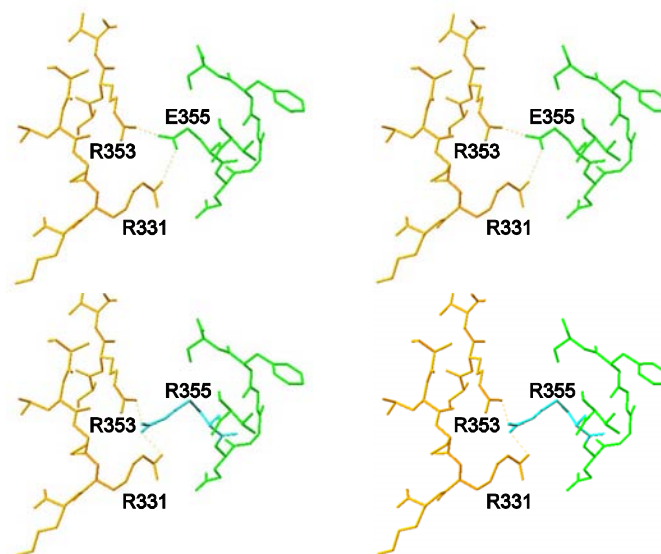


Figure 3

Lattice contacts in wild-type X-ray structure of AspRS-1 (top stereoview) and in model (bottom stereoview) of E355R mutant. All atoms of the wild-type enzyme except the side chain of the mutated residue have been kept in their original places for modelling the lattice contacts of the mutant.

3.3. Disruption of hydrogen bond in packing contacts

Disruption of a hydrogen bond involved in crystal contacts was also investigated. The S360A AspRS-1 variant with mutation of a serine residue involved in such an intermolecular hydrogen bond does not crystallize in the native conditions with sodium formate. This mutated serine participates in wild-type crystals in contacts directly related by the crystallographic 2_1 screw axis parallel to the *b* axis. As shown above, mutation of E355, which is also involved in this type of contact, fails to crystallize. Therefore, the interaction of two dimers related by a 2_1 screw axis seems to be a crucial step in the crystallization process of AspRS-1. Experiments are underway to verify whether such AspRS-1 dimers are the actual building blocks of the orthorhombic crystals.

3.4. Modification of hydrophobic surfaces involved in crystal packing

Two mutants were designed in order to modify the local surface hydrophobicity involved in the crystal contacts. The first one was aimed to decrease a hydrophobic contact by mutating F366 that forms such a contact with L74. By introducing the mutation F366A, the closest distance $A366(C_\beta)\cdots L74(C_\gamma)$ is 4.8 \AA , thereby weakening the hydrophobic contact between AspRS-1 dimers. Crystallization experiments in the presence of sodium formate yielded twinned crystals (Fig. 2e). This could suggest that the intermolecular contact between the two hydrophobic residues F366 and L74 is crucial for

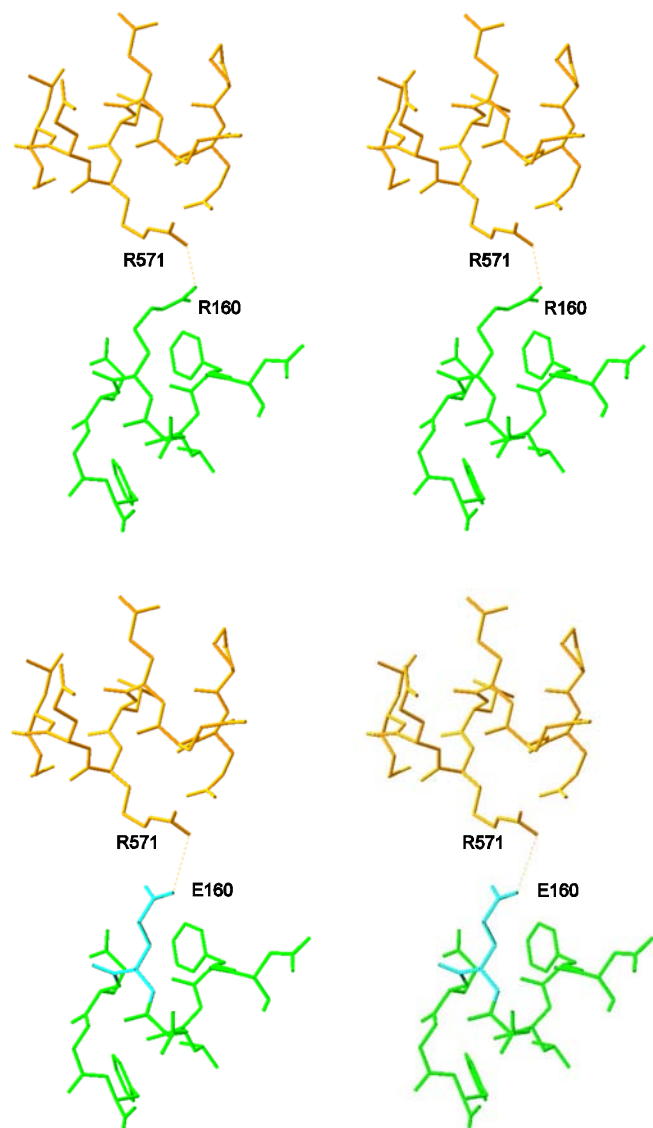


Figure 4

Lattice contacts in wild-type X-ray structure of AspRS-1 (top stereoview) and in model (bottom stereoview) of R160E mutant. Model of mutant is built into the wild-type structure such that crystal contact is formed by ionic interaction between E160 and R571. All atoms of the wild-type enzyme except the side chain of the mutated residue have been kept in their original places for modelling the lattice contacts of the mutant.

crystalline order and that disruption of this contact allows alternative interactions between dimers leading to twinning.

On the contrary, mutant A53I was designed in order to increase hydrophobic crystal contacts. Figure 5 shows the region of the wild-type enzyme around A53, where the crystal contact is formed. The closest distances $A53(C_{\beta})-A373(C_{\beta})$, $A53(C_{\beta})-V370(C_{\gamma1})$ and $A53(C_{\beta})-I305(C_{\beta})$ are 4.5 Å, 4.4 Å, and 5.4 Å, respectively. By introducing the mutation A53I, the existing gap should be bridged and should give rise to improvement of hydrophobic interactions between I53 from one dimer and residues V370, A373 and I305 from another dimer in the crystal. Crystals obtained with this mutant (Fig. 2f) are similar to wild-type crystals and show the same lattice parameters.

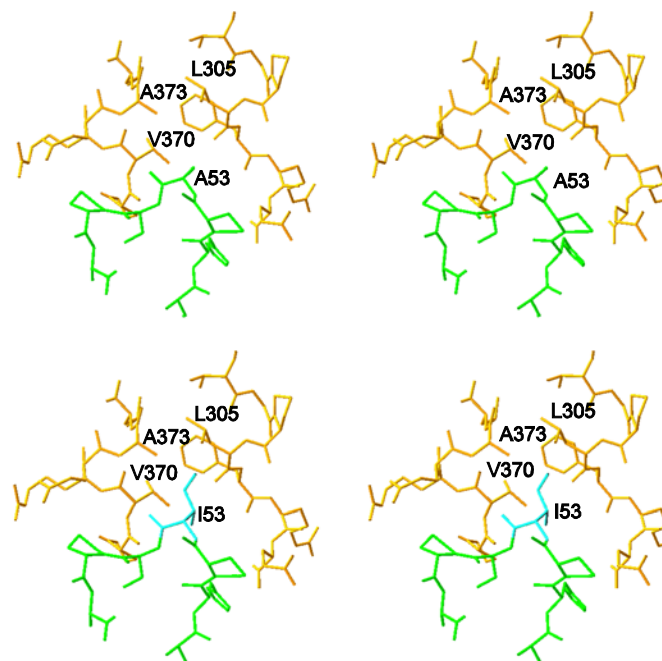


Figure 5

Lattice contacts in wild-type X-ray structure of AspRS-1 (top stereoview) and in model (bottom stereoview) of A53I mutant. Model of mutant is built into the wild-type structure such that a crystal contact is formed by hydrophobic interaction of I53 with residues L305, V370 and A373 from the other molecule. All atoms of the wild-type enzyme except the side chain of the mutated residue have been kept in their original places for modelling the lattice contacts of the mutant.

4. Conclusions

A correlation was found between disruption/addition of intermolecular interactions in the crystal packing and the crystallizability of AspRS-1 mutants: disruption of contacts hinders crystallization and addition of contacts favors it. For instance, disruption of a double salt-bridge formed between dimers being directly related by the crystallographic 2_1 screw axis hinders crystallization in wild-type conditions. Further, disruption of an ionic interaction between dimers related only by a crystallographic translation along the a axis gives clusters of rods instead of single crystals. Twinned crystals were also obtained when a phenylalanine involved in intermolecular hydrophobic contacts is mutated to an alanine. Moreover, an AspRS-1 variant with a serine mutation disrupting an intermolecular hydrogen bond does not crystallize. In contrast when putative crystal contacts are added, as in variant proteins A53I and R160E, well-shaped crystals are obtained.

Experiments are now in progress in order to analyze crystal growth rate, stability and diffraction power of crystals of mutants A53I and R160E, and to compare the behavior of mutant and wild-type crystals. Studying the crystallization of native AspRS-1 will also enable to analyze poisoning effects by structural analogues (mutants) of the crystallizing protein.

We are grateful to the European Commission (BIO4-CT98-0086), CNES, ESA, CNRS and Université Louis Pasteur Strasbourg for continued financial support. CC was supported by EC and CNES.

References

- Becker, H. D., Roy, H., Moulinier, L., Mazauric, M.-H., Keith, G. & Kern, D. (2000). *Biochemistry* **39**, 3216-3220.
- Berchtold, H. & Hilgenfeld, R. (1999). *Biopolymers*, **51**, 165-172.
- Bergfors, T., Rouvinen, J., Lehtovaara, P., Caldentey, X., Tomme, P., Claeysens, M., Petterson, G., Knowles, T. T. & Jones, T.A. (1989). *J. Mol. Biol.* **209**, 167-169.
- Bourguet, W., Ruff, M., Chambon, P., Gronemeyer, H. & Moras, D. (1995). *Nature (London)*, **375**, 377-382.
- Carugo, O. & Argos, P. (1997). *Protein Sci.* **6**, 2261-2263.
- Charron, C., Sauter, C., Zhu, D. W., Ng, J. D., Kern, D., Lorber, B. & Giegé, R. (2001). *J. Cryst. Growth*, **232**, 376-386.
- Delarue, M., Poterszman, A., Nikonov, S., Garber, M., Moras, D. & Thierry, J.-C. (1994). *EMBO J.* **13**, 3219-3229.
- Green, M. E., Kirkland, N. & Ng, J. D. (2001). *J. Cryst. Growth*, **232**, 387-398.
- Heinz, D. W. & Matthews, B. W. (1994). *Protein Eng.* **7**, 301-307.
- Janin, J. (1997). *Nature Struct. Biol.* **4**, 973-974.
- Kunkel, T. A. (1985). *Proc. Natl Acad. Sci. USA*, **82**, 488-492.
- Lawson, D. M., Artymiuk, P. J., Yewdall, S. J., Smith, J. M. A., Livingstone, J. C., Treffy, A., Luzzago, A., Levi, S., Arosio, P., Cesareni, G., Thomas, C. D., Shaw, W. V. & Harrison, P. M. (1991). *Nature*, **349**, 541-544.
- McElroy, H. E., Sisson, G. W., Schoettlin, W. E., Aust, R. M. & Villafranca, J. E. (1992). *J. Cryst. Growth*, **122**, 265-272.
- Mittl, P. R. E., Berry, A., Scrutton, N. S., Perham, R. N. & Schulz, G. E. (1994). *Acta Cryst. D***50**, 228-231.
- Ng, J. D., Lorber, B., Witz, J., Théobald-Dietrich, A., Kern, D. & Giegé, R. (1996). *J. Cryst. Growth*, **168**, 50-62.
- Ng, J. D., Sauter, C., Lorber, B., Kirkland, N., Arnez, J. & Giegé, R. (2002). *Acta Cryst. D***58**, 645-652.
- Otwinowski, Z. & Minor, W. (1996). *Methods Enzymol.* **276**, 307-326.
- Sauter, C., Lorber, B., Cavarelli, J., Moras, D. & Giegé, R. (2000). *J. Mol. Biol.* **299**, 1313-1324.
- Sauter, C., Lorber, B., Théobald-Dietrich, A. & Giegé, R. (2001). *J. Cryst. Growth*, **232**, 399-408.
- Waller, J.-P., Risler, J.-L., Monteilhet, C. & Zelwer, C. (1971). *FEBS Lett.* **16**, 186-188.